Geoscience Frontiers xxx (2016) 1–13

HOSTED BY

ELSEVIER

Contents lists available at ScienceDirect

China University of Geosciences (Beijing)

Geoscience Frontiers

journal homepage: www.elsevier.com/locate/gsf

Research paper

Extraterrestrial microspherules from Bajada del Diablo, Chubut, Argentina

M.J. Orgeira [a,b,*], L.N. Castro [a,c], G.A. Goldmann [a], C.B. Prezzi [a,b], E. Sileo [d], D.R. Vega [e], C. Franzosi [a], R.D. Acevedo [f], O. Martínez [g], J. Rabassa [f,h], J.F. Ponce [f,h], O.R. Tófalo [a]

[a] Departamento de Ciencias Geológicas-IGEBA, Facultad de Ciencias Exactas y Naturales, Universidad de Buenos Aires, Ciudad Universitaria, Pabellón II, C1428EHA, Buenos Aires, Argentina
[b] Consejo Nacional de Investigaciones Científicas y Técnicas de Argentina, CONICET, Argentina
[c] Departamento de Ingeniería Agrícola y Uso de la Tierra, Facultad de Agronomía, Universidad de Buenos Aires, Av. San Martín 4453, C1417DSE, Buenos Aires, Argentina
[d] INQUIMAE, Departamento de Química Inorgánica, Analítica y Química Física, Facultad de Ciencias Exactas y Naturales, Universidad de Buenos Aires, Pabellón II, Ciudad Universitaria, C1428EHA, Buenos Aires, Argentina
[e] Gerencia de Investigación y Aplicaciones, Comisión Nacional de Energía Atómica, Universidad Nacional General San Martín, Buenos Aires, Argentina
[f] Centro Austral de Investigaciones Científicas, CADIC-Conicet, Ushuaia, Argentina
[g] Universidad Nacional de la Patagonia "San Juan Bosco" Sede Esquel, Chubut, Argentina
[h] Universidad Nacional de la Patagonia "San Juan Bosco" Sede Ushuaia, Ushuaia, Argentina

ARTICLE INFO

Article history:
Received 4 August 2015
Received in revised form
17 December 2015
Accepted 4 January 2016
Available online xxx

Keywords:
Extraterrestrial microspherules
Chemistry
Bajada del Diablo
Chubut
Patagonia-Argentina

ABSTRACT

The Quaternary infilling of a circular structure located in Bajada del Diablo, Chubut Province, Argentina has been proposed as a crater strewn field in previous studies. Here we report the finding of about 65 microspherules collected in a trench excavated in the center of the structure. The majority of hand-picked specimens are single, but some of them exhibit compound forms. The single specimens are spherical with a mean size of 137 μm, whereas the more complex samples show peduncles and drop shapes. Dendritic crystal growth is recognized in the internal structure of some broken microspherules. Preliminary chemical composition from the surface and center of microspherules was determined by energy dispersive spectrometry employing EDS. Quantitative EMPA and XRD analysis indicate that the microspherules are mainly composed of Fe and O with magnetite, Fe° with subordinate wüstite. Following consideration of possible anthropogenic and volcanic origins, these spherulites are ascribed to an extraterrestrial input. An accumulation rate of 47 microspherules per m^2/yr is estimated for the studied sediments. This value is two orders of magnitude higher than the reference flux for cosmic dust estimated for the last 1 Ma in the Transantarctic Mountains. The microspherules might have been generated as a byproduct of asteroid entry in the atmosphere.

1. Introduction

In the northern Patagonian Massif of Chubut Province in Argentina (Fig. 1), the two main units exposed are the Quiñelaf Eruptive Complex and the Pampa Sastre Formation. The Quiñelaf Eruptive Complex is mainly composed of trachytes with subordinate rhyolites, trachyandesites, trachybasalts, and pyroclastic rocks. Based on several radiometric data, the latest volcanic activity of this trachytic unit is inferred as late Miocene (Ardolino, 1981). The Pampa Sastre Formation is represented by conglomerate layers with basalt boulder clasts in a coarse sandy matrix. The presence of interbedded calcic layers has been described near the top. These sediments are compositionally and texturally very immature, suggesting short and fast transportation. Ardolino and Franchi (1996) assigned this unit to the Pliocene–early Pleistocene. Degradation of the landscape under an arid/semiarid cold climate produced these gravel and sand deposits. A general uplift of the area, and a consequent relative

* Corresponding author. Departamento de Ciencias Geológicas-IGEBA, Facultad de Ciencias Exactas y Naturales, Universidad de Buenos Aires, Ciudad Universitaria, Pabellón II, C1428EHA, Buenos Aires, Argentina.
E-mail address: orgeira@gl.fcen.uba.ar (M.J. Orgeira).
Peer-review under responsibility of China University of Geosciences (Beijing).

http://dx.doi.org/10.1016/j.gsf.2016.01.004

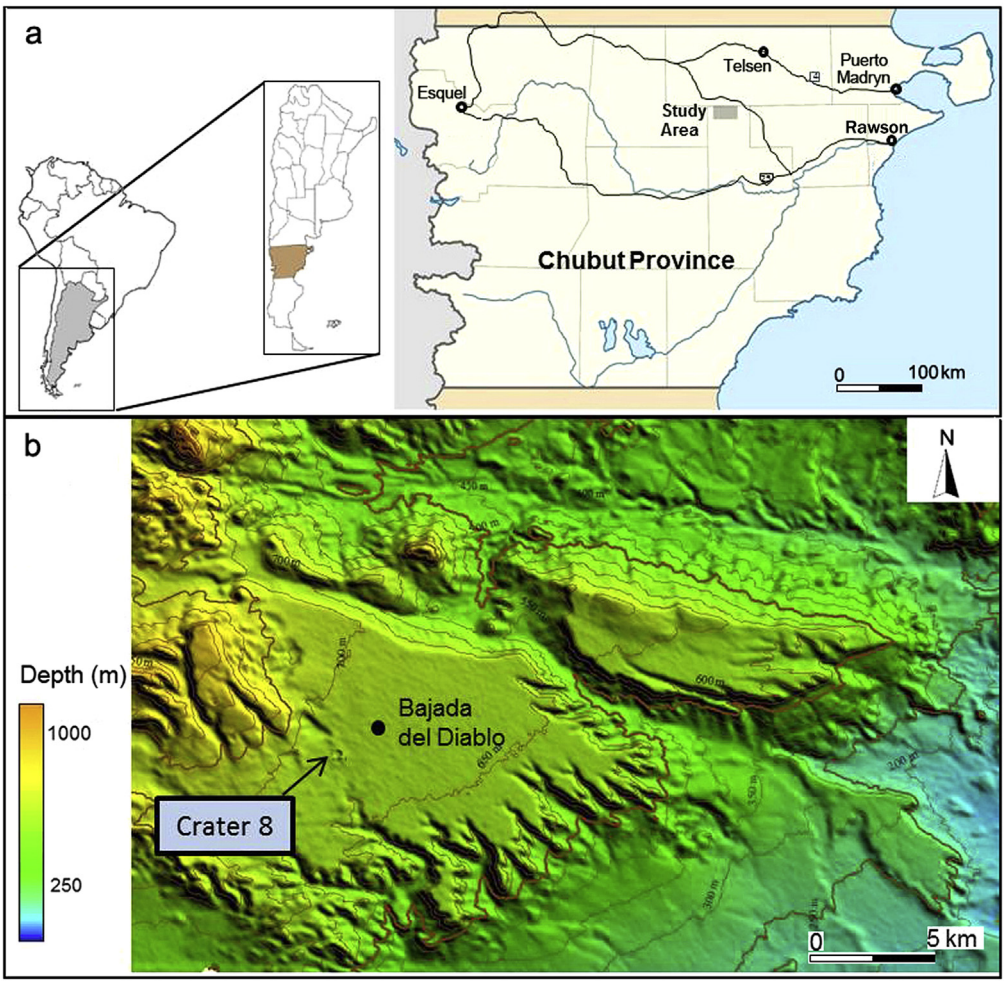

Figure 1. Location of the study area. The point indicates *Crater 8* site.

decline of the base level took place in the late Pleistocene. Subsequently, erosive and sedimentary processes generated three accumulation surfaces around the core of this Patagonian massif (Ardolino and Franchi, 1996).

A volcanic plateau formed by successive lava flows is the most important geomorphological feature in the area while later fluvial and gravity processes sculpted this landform (González Díaz and Malagnino, 1984; Ardolino, 1987).

Based on remote sensing analyses and field studies, Acevedo et al. (2009, 2012) hypothetically ascribed Bajada del Diablo area to a crater strewn field. According to these authors, an extraterrestrial impactor would have targeted on the Miocene eruptive Complex Quiñelaf, on the late Pliocene/early Pleistocene Pampa Sastre Fm. and the Pleistocene alluvial sediments. The observed circular structures are simple bowl-shaped craters with high apparent depth/diameter ratios, characterized in some cases by a raised rim. These craters have been partially filled in recent times by diamictic sediments from the rims and windblown sands.

Acevedo et al. (2009, 2012) proposed that the origin of this crater field might be related to the multiple fragmentation of one asteroid of "rubble pile" structure that broke up before impact; as an alternative hypothesis, they suggested a collision of a split comet. This event would have occurred between early Pleistocene and late Pleistocene i.e., 0.78–0.13 Ma ago (Acevedo et al., 2009, 2012).

Prezzi et al. (2012, 2013, 2016) carried out detailed topographic, magnetic and electromagnetic ground surveys in the two circular structures found in Pampa Sastre conglomerates. The magnetic anomalies show a circular pattern with magnetic lows at the bottom of the structures. Furthermore, near the rims, high-amplitude, conspicuous and localized (short wavelength) anomalies were also observed. Such large amplitude and short wavelength anomalies are not detected outside the circular structures. For all the employed frequencies, the electromagnetic profiles show lower apparent electrical conductivities at the floor of the structures, while at the rims, the signals possess notably higher values. The authors suggested that at the bottom up to 12 m of Pampa Sastre conglomerate would have been removed. On the hand, at the rim of the circular structure with high-amplitude, localized magnetic anomalies and higher apparent electrical conductivities are present, which would be related to the anomalous accumulation of basalt boulders and blocks which were permanently magnetized. The fact that such high-amplitude anomalies are not present outside the surveyed circular structures, together with geomorphological, geological and the other geophysical features of the studied circular structures, support the hypothesis of an extraterrestrial projectile impact.

Although Bajada del Diablo was proposed as one of the largest crater strewn fields in the world (Acevedo et al., 2012), taking into account its extension and the number of alleged impact structures including ca. >80 circular or elliptical features with a

Please cite this article in press as: Orgeira, M.J., et al., Extraterrestrial microspherules from Bajada del Diablo, Chubut, Argentina, Geoscience Frontiers (2016), http://dx.doi.org/10.1016/j.gsf.2016.01.004

30 km × 12 km dispersion, the region is still under investigation and debate. The raised rims of Pampa Sastre Fm. sequences with morphological and geophysical signatures in accordance with the criteria of Grieve and Pilkington (1996) further characterize these structures.

In this contribution, we analyze the nature of the Quaternary infilling of one of these structures (*Crater 8 sensu* Acevedo et al., 2009), located at 42°46′43″S, 67°24′45″W. We also evaluate the evidence for a possible impact (Fig. 1).

2. Materials and methods

In a previous survey, the topography of the *Crater 8* (*sensu* Acevedo et al., 2009) revealed a diameter of ca. 300 m with an apparent depth of 16 m (Prezzi et al., 2012; Fig. 2). A 2 m long and 1.2 m depth trench was dug in the center of circular *Crater 8* (Fig. 3). Representative samples of ~2.5 kg were collected from all recognized units and described. As the samples were slightly consolidated, effective disaggregation was completed using a porcelain mortar and a rubber pestle avoiding grain breakage.

The magnetic susceptibility of each sample was measured using a Bartington suceptibilimeter MS2 at Instituto de Geociencias Básicas y Aplicadas, Faculty of Exact and Natural Sciences, University of Buenos Aires (IGeBA, FCEN, UBA).

All samples were treated with 10% HCl in order to eliminate carbonate cements and other calcareous debris as fine grained carbonates and calcrete horizons were extensively present in the studied section. Samples were washed with distilled water over a 62 μm Tyler sieve to retain the sandy fraction for further binocular magnifying glass examination. As observations revealed the presence of microspherules in some samples, hand picking was carried out for separating them. Selected specimens were placed on conductive copper and carbon sticky tapes mounted on a circular aluminum sample holder. Scanning electron microscopy was carried out using a SEM Zeiss Supra 40 microscope equipped with a field emission gun at Centro de Microscopía Avanzada, CMA, University of Buenos Aires. Images were taken with in-lens detector and 5 kV acceleration voltages for textural and size analysis. Semi-quantitative elemental composition of microspherules was determined by energy-dispersed spectrometry (EDS) using an Oxford Instruments Detector at the CMA.

Additionally, key-samples were analyzed by XRD and EMPA techniques.

The mineral chemistry of the various phases in a selection of microspherules was obtained by electron probe microanalyses

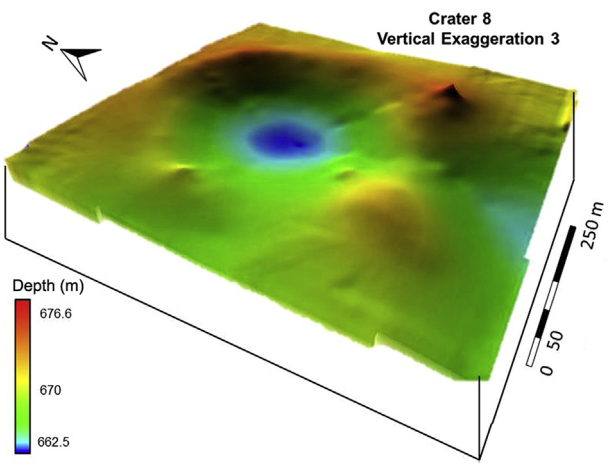

Figure 2. Detailed topography of *Crater 8* surveyed using a total station. Modified from Prezzi et al. (2012).

Figure 3. Exposed profile inside the 2 m depth trench dug in *Crater 8*.

(EPMA) using a JEOL JXA 8230 electron microprobe at LAMARX (Universidad Nacional de Córdoba, Argentina). Instrument conditions were 15 kV accelerating voltage, 10–20 nA beam current, and 4–6 μm nominal beam spots. Standards used for instrumental calibration were natural minerals (anorthoclase, anorthite, chromite, fayalite, ilmenite, periclase, nickeline and rhodonite) and pure elements (Fe, Ni, Co, Ir, Os, Pd, Pt, Rh and Ru).

XRD data were obtained using single crystal and XRPD techniques. A single crystal diffractometer with an EOS CCD detector, by means of CrysAlis PRO (Oxford Diffraction, 2009) was used applying Mo radiation. Sample was mounted with oil using a standard loop. Diffraction data were collected as triclinic system (reciprocal hemisphere). Two different samples were examined, 278 and 336 frames using 1deg ω-scan, of two microspherules (samples 8.23 and 8.24). As the beam passed through the body of the diffracting spherule, this technique allowed the individual characterization of the entire sample without damaging the specimen. After collecting the data, the obtained diffractions points were transformed to a powder diagram using the "powder power tool" command. X-ray powder diffraction data were obtained using an Oxford Diffraction Gemini.

3. Results

The exposed sedimentary profile shows two units labeled from bottom to top as unit B and unit A separated by an abrupt erosive appearance contact where vertical cracks could be recognized (Fig. 4).

The basal unit B is represented by a 70 cm yellowish gray (5Y 8/1) horizon whose calcium carbonate content increases to the top. Subparallel and diffuse lamination could be recognized. Calcite growth generates floating textures where sand and sabulite grains (<1 mm in diameter) are dispersed. Microscopic observations revealed a laminar microstructure defined by micrite bands. The c/f 20 μm related distribution is open porphyric. The clasts are mainly composed of microlithic fragments, mono and polycrystalline quartz, chalcedony, plagioclase, potassium feldspar and heavy minerals (pyroxene, amphibole and opaque). A micritic calcite

Please cite this article in press as: Orgeira, M.J., et al., Extraterrestrial microspherules from Bajada del Diablo, Chubut, Argentina, Geoscience Frontiers (2016), http://dx.doi.org/10.1016/j.gsf.2016.01.004

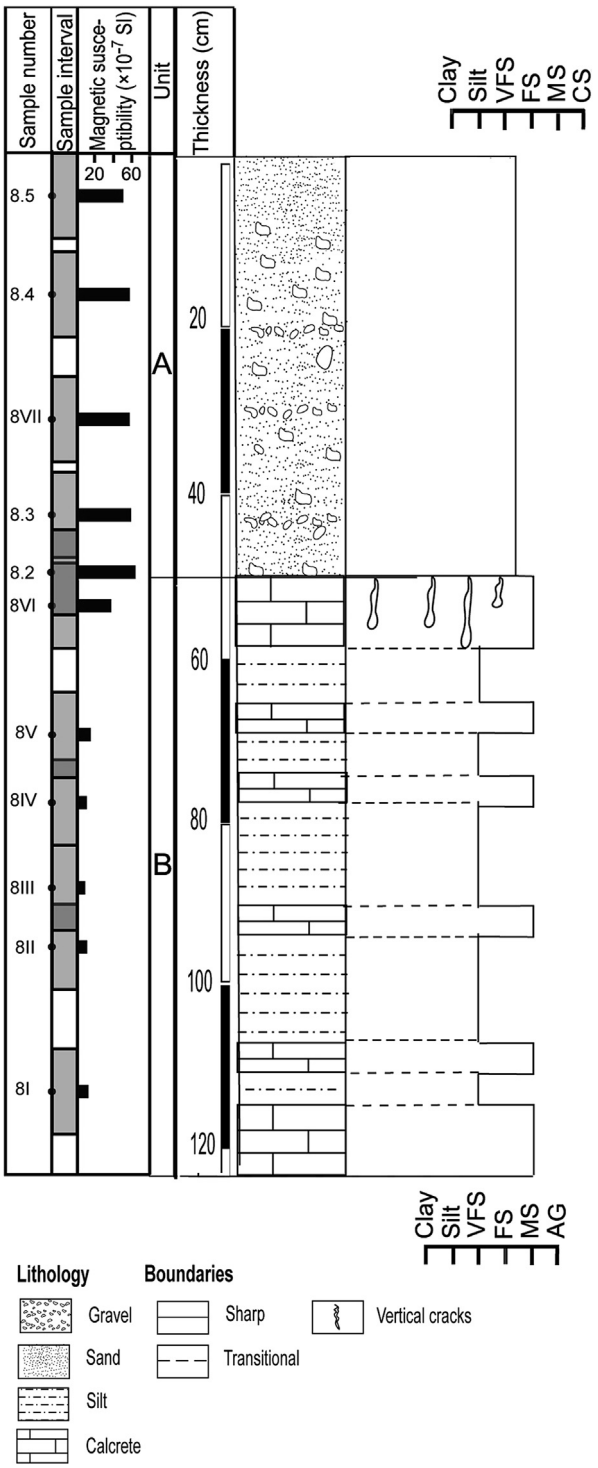

Figure 4. Schematic stratigraphic profile exposed in center of *Crater 8*.

determines a cristalithic b-fabric (Fig. 5). Pedofeatures consist of carbonate particles, including spherical pellets, some of them concentrically laminated and ooids (Fig. 5), classifying the rock as a pedogenic calcrete (Hay and Wiggins, 1980; Narayan and Tandon, 1981; Wright, 1983; Alonso-Zarza and Wright, 2010). The observed characteristics are very similar to those described by Bouza (2012) in petrocalcic horizons (2Bkm) of Petrocalcids of river terraces RP1 (155 m above sea level) and RP2 (137 m above sea level), to the northeast of the Chubut province, Argentina, where a

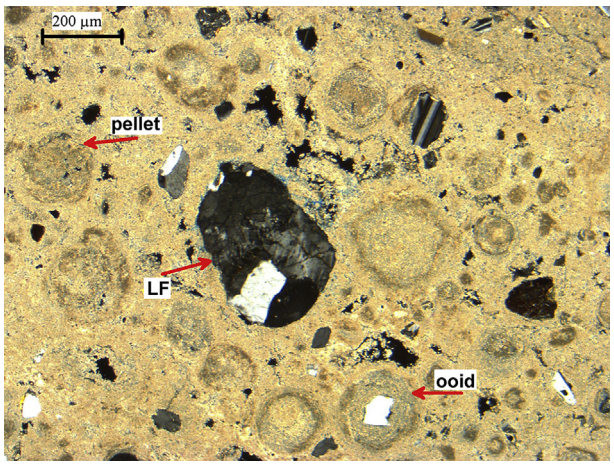

Figure 5. Microscopic thin section of a pedogenic calcrete horizon, top of unit B. The clasts are mainly composed of microlithic fragments. A micritic calcite determines a cristalithic b-fabric. Pedofeatures: carbonate particles, including spherical pellets.

time correlation of these petrocalcic horizons with the Marine Isotope Stage 5 has been suggested based on mineralogical and climatic considerations.

The uppermost unit A is represented by a pale brownish (5YR 7/1), homogeneous diamictic deposit 55 cm thick, composed of a silty/sandy matrix with ~2 cm diameter poorly rounded light brown basalt pebbles ca 10–15% of total volume. The volumetric magnetic susceptibility of collected samples is represented in Fig. 4. A pronounced increase of magnetic susceptibility in the diamictic material is observed; followed by a gradual and moderate decrease toward the top. The signal is compatible with a higher amount of magnetic minerals, gradually decreasing towards the top. This variation can also be related to a decrease in magnetic particles grain size from base to top of the upper unit (Dunlop and Özdemir, 1997).

The samples containing microspherules are located over the sharp contact between the pedogenic calcrete of unit B and the diamictic sediments of unit A (samples 8.2–8.3 in Fig. 4).

A total of ~65 spherical microspherules ranging in diameter from 88 to 300 μm were recovered from the lower part of unit A. Appendix 1 shows all recovered microspherules. The majority of hand-picked specimens are single spherical forms, whereas some are compound forms. The others show peduncles and drop shapes (Fig. 6). A dendritic crystal growth was recognized in the internal structure of broken individuals (Fig. 7).

Microspherules display a symmetric unimodal granulometric distribution with a mean fraction generally between 125 and 250 μm size (Fig. 8a). Although the microspherules exhibit different surface morphologies, most of them have a polygonal texture with interlocking crystals (Figs. 8b and 9). Smooth surfaces with no significant changes in geometry, protrusions and brain or skein types with brick-work patterns are also identified (Fig. 10). EDS surface chemical analysis of the microspherules reveals Fe and O as major constituents with subordinate C, Si, Ca and Al. Among other trace elements Dy, V, Mn and Ti are also detected (Table 1). Chemical composition of the microspherules vs. size is represented in Fig. 11.

The crystal composition of the collected microspherules in the powder diagrams determined by XRD shows that the main peaks in both samples correspond to a major spinel phase (magnetite, PDF 19/0629). However, small differences can be found between the signals of the two samples (Figs. 12 and 13).

Please cite this article in press as: Orgeira, M.J., et al., Extraterrestrial microspherules from Bajada del Diablo, Chubut, Argentina, Geoscience Frontiers (2016), http://dx.doi.org/10.1016/j.gsf.2016.01.004

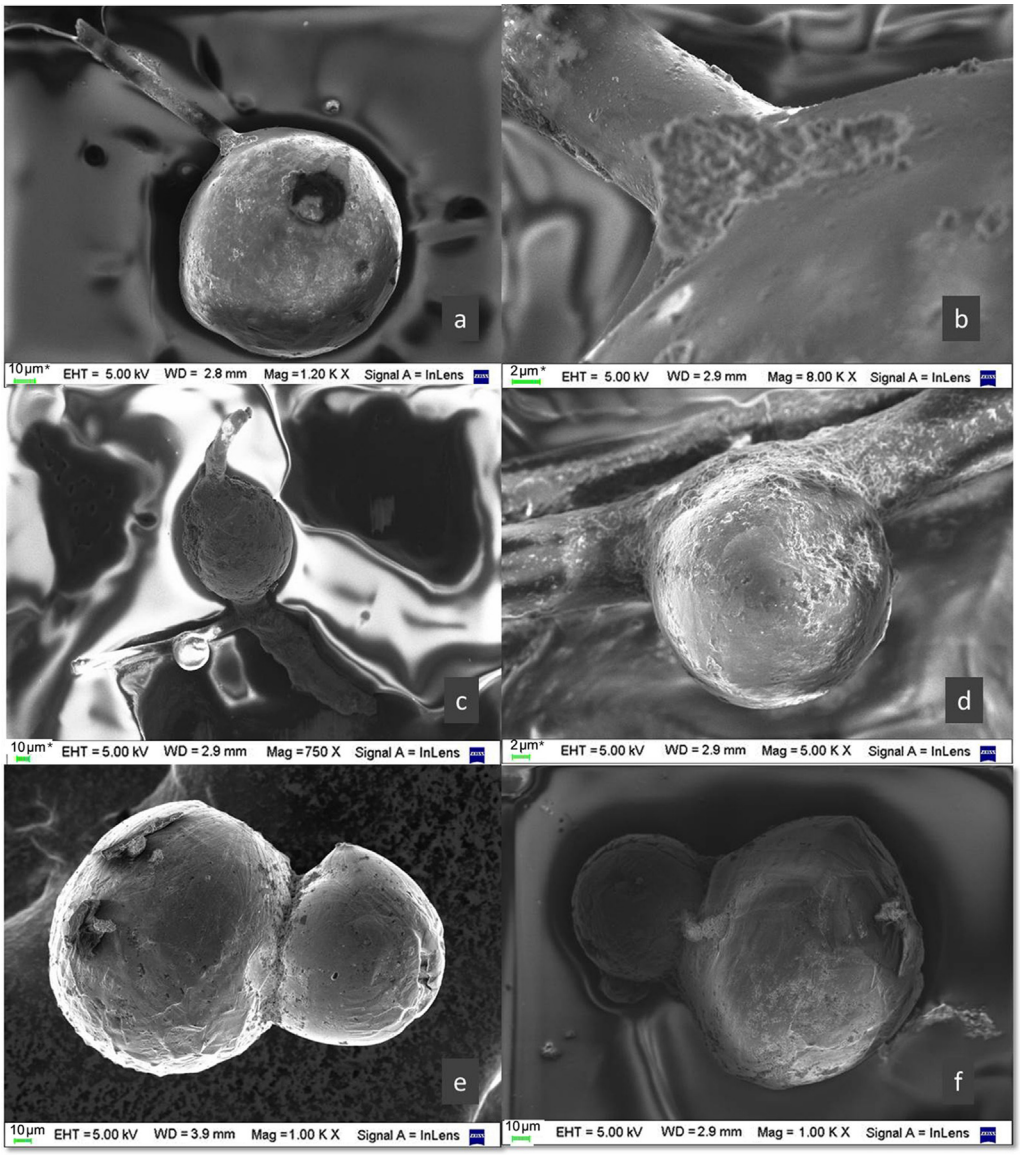

Figure 6. Electron microscope photomicrographs of the microspherules. The majority have a spherical shape with occasional siliceous peduncles (a, b, c and d). Single and compound forms (e and f) are observed.

Meanwhile sample 8.23 (see Appendix 1) displays shoulders and weak peaks. Sample 8.24 (Fig. 13) exhibits a simple feature which represents practically only magnetite. In Sample 8.23, additional signals at 19.18, 27.20, 33.29 and 42.22° could be assigned to wüstite (PDF 46-1312). On the other hand, the weak peak at 20.41° in the same sample could indicate the presence of Fe° (PDF 87-0721). Sample 8.24 also displays weak and wide signals at 17.82 and 21.76° that are not present in sample 8.23, and could not be assigned. The mineralogy detected by X ray is in agreement with atomic percentages obtained by EDS technique.

Table 2 shows EDS analysis of two broken microspherules taking into account different spot areas for each specimen (samples 8.36 and 8.66). The internal structure observed with backscattered diffraction exhibits a polygonal patterned surface compatible with a dendritic crystal intergrowth of mainly Fe and subordinate C phases (Fig. 14).

Selected microspherules were sectioned and polished for EMPA analyses. Data from two samples were obtained (five measurements in total, two from one and three from the other one). Table 3 shows the microprobe results with their respective standard deviations. The results show the following elements. *Microspherule 1* contains mostly Fe and small percentages of Si and Al; although the concentration of the subordinate elements is very low, they vary markedly in the two analyzed spots. Three different zones were measured in *Microspherule 2*, with Fe as the major element. Also, Al, Si, Ti and Mg were detected in small quantities. Ti concentration was similar in all spots and only one measurement revealed the presence of small quantities of Mg.

In summary, the results described above show that the microspherules possess dendritic internal structure, and compositional intergrowth of predominantly magnetite and subordinate wüstite, with interstitial metallic iron and an undetermined phase that include carbon.

4. Discussion

Acevedo et al. (2012) found four Fe-Ni lawrencite-bearing microspherules of 300 µm in average diameter, presumably

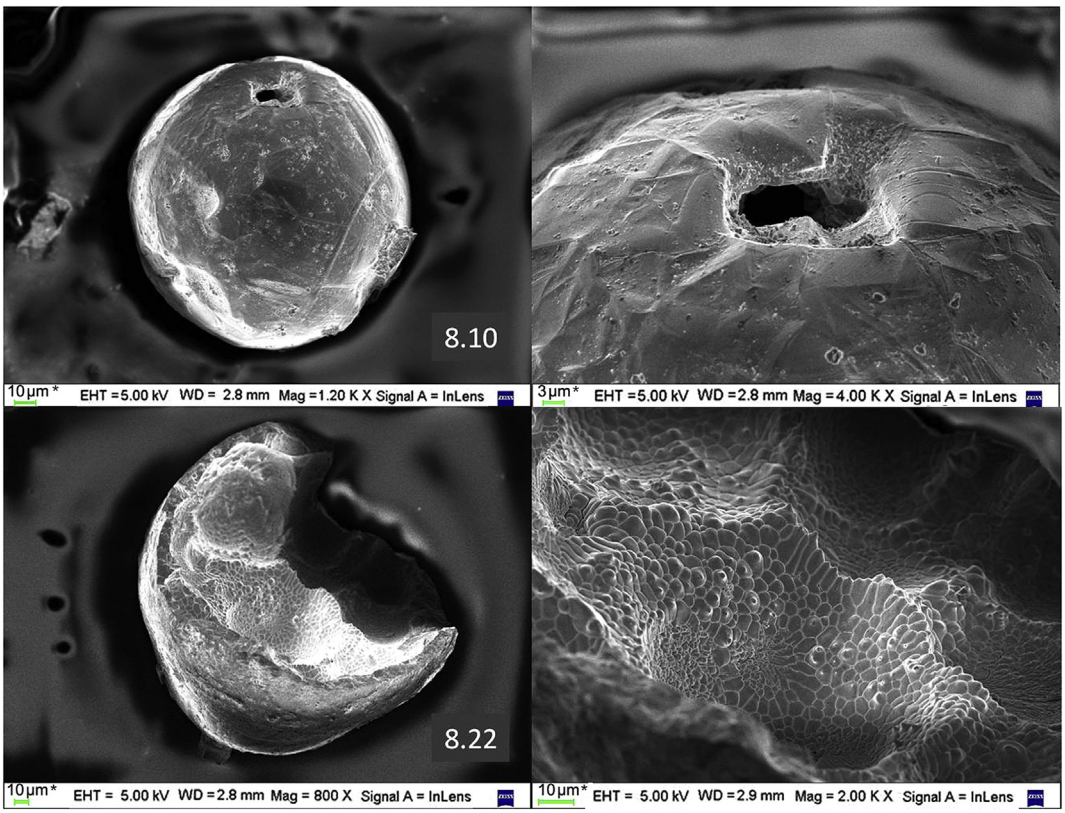

Figure 7. Details of the internal texture of two selected microspherules: sample 8.10 top right and left show an apparently inwards indentation whereas sample 8.22 bottom right and left exhibit a hollow with dendritic crystal growth.

originated by the impact, buried under post-impact sedimentary coverage. The composition allowed them to suggest a potential contamination with Cl during atmospheric entry. However, these microspherules are not included in the following discussion due to different methodology of treatment of the samples.

Several mechanisms are proposed for the origin of nano and microspherules in the literature. Their genesis can be attributed as terrestrial byproduct of volcanism or anthropogenic activities and on the other hand, to three possible sources of extraterrestrial matter: (1) recrystallized cosmic dust; (2) meteor ablation or (3) the direct result of a crater impact process as dissipated melt drops (French and Koeberl, 2010).

Carracedo Sánchez et al. (2015) reported microparticles associated with explosive phase eruptions related to basaltic volcanism. These volcanic microspherules exhibit a siliceous composition, irregular shape, and larger average diameters around 1 mm. The microspherules discussed in this contribution cannot be linked to such processes due to the notable texture, size and compositional differences in comparison to those of volcanic origin.

The studied area is an isolated region. There are no major roads, with only a few tracks. The nearest industrial factory area (Aluar, Puerto Madryn, Chubut Province) is located 200 km eastward. Moreover, the prevailing winds in the area are S–SW; consequently pollution in the vicinity is unlikely. Furthermore, the external

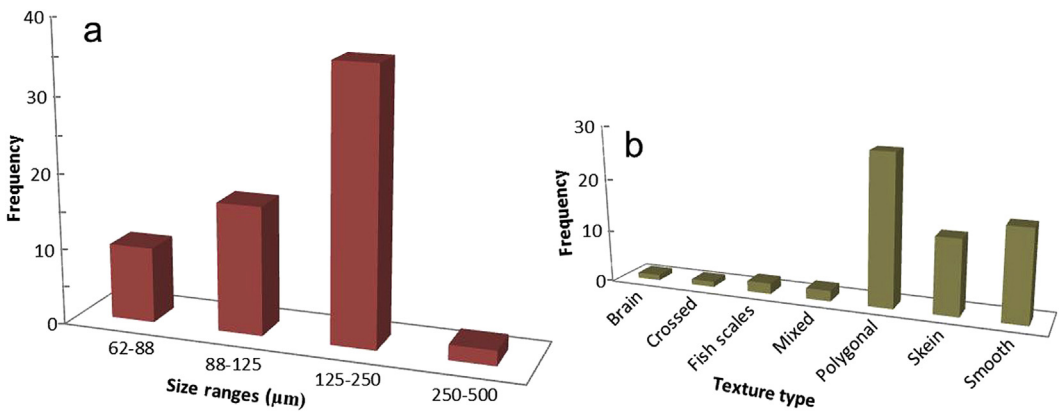

Figure 8. (a) Frequency versus size of spherules. Mean fraction is located between 125 and 250 µm sizes. (b) Frequency versus surface texture type. Polygonal textures are the most common in the analyzed samples.

Please cite this article in press as: Orgeira, M.J., et al., Extraterrestrial microspherules from Bajada del Diablo, Chubut, Argentina, Geoscience Frontiers (2016), http://dx.doi.org/10.1016/j.gsf.2016.01.004

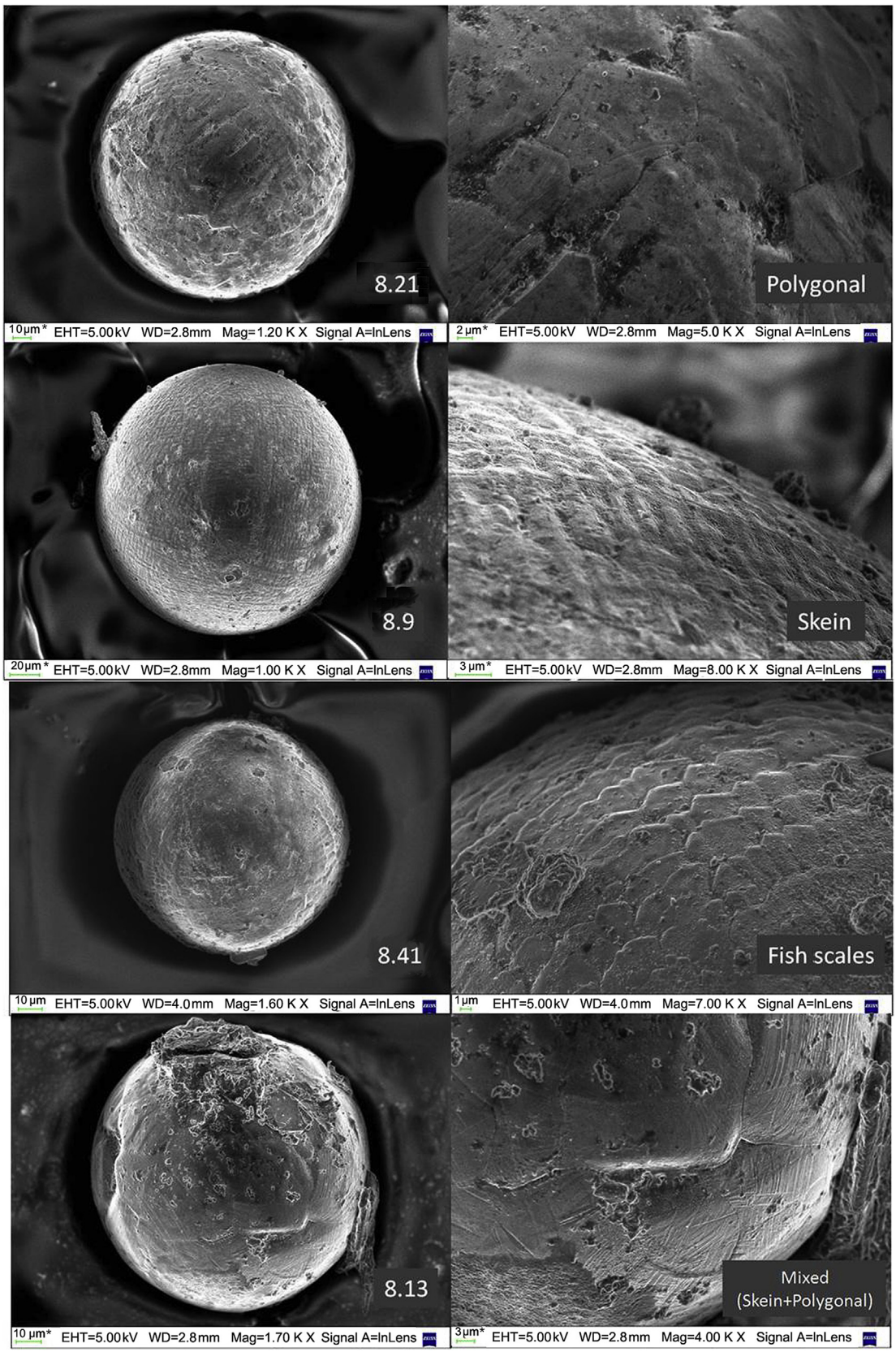

Figure 9. Detailed images of external texture patterns. The polygonal texture is an interlocking arrangement of dendritic crystals. Skein type is determined by filigree like patterns with dendritic fine crystals. Fish scales are defined by the overlapping of crystals with sharp boundaries facing outwards. Mixed is a composite type in which across the surface of a polygonal crystal a filigree pattern could also be identified.

Please cite this article in press as: Orgeira, M.J., et al., Extraterrestrial microspherules from Bajada del Diablo, Chubut, Argentina, Geoscience Frontiers (2016), http://dx.doi.org/10.1016/j.gsf.2016.01.004

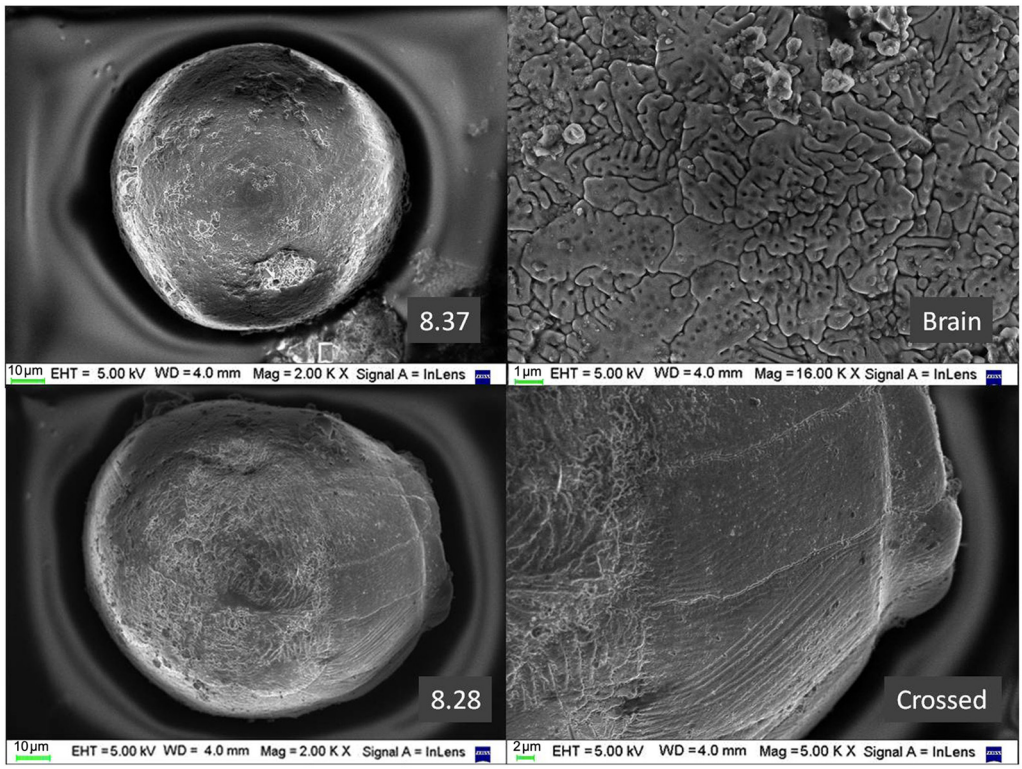

Figure 10. Detailed images of external texture patterns. Top: Brain texture is determined by a fine dendritic crystal growth. Bottom: Crossed type texture defined by distinctive filigree like patterns with two dominant directions superimposed over a single crystal.

texture of the spherules produced by industrial combustion has characteristic, "orange-peel" features (Maher et al., 1999; Evans and Heller, 2003). Considering the location of the studied area, and the textures observed in the collected material, an anthropogenic origin is also excluded, and support an extraterrestrial origin.

Microspherules with different composition and size have been previously documented in crater strewn fields such as Macha, Russia (Gurov and Gurova, 1998), Kaali Island, Estonia (Raukas, 2004) and Morasko, Poland (Stankowski et al., 2006; among others).

Chemical composition showed no significant changes with respect to particle size (Fig. 11). Most of the microspherules are mainly composed of Fe and O. Minor elements such as C, Si, Ca, Y, Al, and Dy could be derived from the calcrete substrate and/or clasts of alumina-silicate basic rocks from Pampa Sastre Fm. Cl and Na are related to surface mineral overgrowths produced by recent exogenous processes. Conspicuous higher silica content in peduncles, in contrast to lower values of surface composition of the microspherule, could be attributed to differentiation processes during crystallization.

According to the chemical composition, mostly composed of FeO (Table 1), the *Crater 8* microspherules were classified as I-type following Genge et al. (2008) criteria. The XRD and EMPA data show magnetite-wüstite and possible metallic iron intergrowths (Figs. 12 and 13 and Table 3). I-type microspherules are present in deep sea collections; however, they constitute only 2% of 1600 cosmic particles collected at the bottom of the South Pole Water Well (Taylor et al., 2000). The composition of these microspherules was attributed by other authors to an extraterrestrial origin (Marini et al., 2004; Genge et al., 2008; Folco et al., 2015; among others). As mentioned previously, most of the findings correspond to single microspherules, but compound forms analogous to those described by Marini et al. (2004) from Kaali crater field in Estonia, were also detected.

In order to compare with the current normal flux of cosmic input, an estimation of the microspherules concentration was carried out, taking into account the horizon with the highest number of particles (Unit A – sample 8.2). Considering a collected sample weight of 2.5 kg, loess density of 2.200 kg/m^3 and a typical deposition rate for this type of sediment of 14 mm/1000 yr (minimum estimative rate of deposition for eolian silts, Valencio et al., 1987), an accumulation rate of 47 microspherules per m^2/yr was estimated. This value is two orders of magnitude higher than the reference flux presented by Rochette et al. (2008) for the last 1 Myr in the Transantarctic Mountains (0.17 spherulites per m^2/yr). Furthermore, *Crater 8* microspherules double the estimated values documented by Voldman et al. (2013) for the Ordovician of Argentina, (9.2–19.6) $\times$ 10^6 per m^2/Myr, which is considered an anomalous microspherule flux. Therefore, the very high anomalous concentration of *Crater 8* microspherules seems not to be related to cosmic dust input through the atmosphere.

Blanchard et al. (1978) proposed a mechanism of microspherule genesis based on observations in samples recovered from oceanic abyssal clays. Microspherules were formed as melted particles, and then progressively recrystallized following separation from the parental meteoritic bodies. In the case of iron meteoroid bodies, metal oxidation can produce wüstite, magnetite and occasionally hematite.

Examples of microspherules formed in terrestrial impact events, as droplets of glass and melted meteoritic metal, are related with young and well-preserved impacts craters. Moreover, microspherules are increasingly recognized as an important component of the distal ejecta layer from impact structures, and they may be found at great distances from the impact site (French, 1998).

Please cite this article in press as: Orgeira, M.J., et al., Extraterrestrial microspherules from Bajada del Diablo, Chubut, Argentina, Geoscience Frontiers (2016), http://dx.doi.org/10.1016/j.gsf.2016.01.004

Table 1
Size, texture and chemical composition (in wt.%) of the collected micro spherules.

Sample	Size (μm)	Text	Fe	O	C	Si	Ca	Al	Na	Cu	Cl	Dy	Mn	K	S	Mg	Ti	V
8.1	150	P	57.8	34.7	3.0	0.0	0.0	0.0	0.0	0.0	0.0	4.6	0.0	0.0	0.0	0.0	0.0	0
8.2	150	P	58.3	32.8	3.7	0.0	0.0	0.3	0.0	0.0	0.0	4.6	0.3	0.0	0.0	0.0	0.0	0
8.3	100	Sk	63.9	28.7	3.4	0.0	0.0	0.0	0.0	0.0	0.0	4.0	0.0	0.0	0.0	0.0	0.0	0
8.4	81	Sk	64.6	30.2	4.5	0.3	0.0	0.4	0.0	0.0	0.0	0.0	0.0	0.0	0.0	0.0	0.0	0
8.5	145	P	67.0	29.3	3.7	0.0	0.0	0.0	0.0	0.0	0.0	0.0	0.0	0.0	0.0	0.0	0.0	0
8.6	74	Sk	54.3	38.5	7.2	0.0	0.0	0.0	0.0	0.0	0.0	0.0	0.0	0.0	0.0	0.0	0.0	0
8.7	125	Sm	56.6	35.8	6.5	0.3	0.9	0.0	0.0	0.0	0.0	0.0	0.0	0.0	0.0	0.0	0.0	0
8.8	160	Sk	60.1	33.4	5.4	0.7	0.5	0.0	0.0	0.0	0.0	0.0	0.0	0.0	0.0	0.0	0.0	0
8.9	170	sk	69.6	27.5	2.9	0.0	0.0	0.0	0.0	0.0	0.0	0.0	0.0	0.0	0.0	0.0	0.0	0
8.10	110	P	63.7	33.4	3.0	0.0	0.0	0.0	0.0	0.0	0.0	0.0	0.0	0.0	0.0	0.0	0.0	0
8.11	120	Sk	62.8	7.4	28.1	0.0	0.0	0.2	0.0	1.5	0.0	0.0	0.0	0.0	0.0	0.0	0.0	0
8.12	100	Sm	63.8	31.2	4.2	0.0	0.0	0.8	0.0	0.0	0.0	0.0	0.0	0.0	0.0	0.0	0.0	0
8.13	100	Mx	59.8	34.9	4.3	0.0	0.0	0.3	0.0	0.8	0.0	0.0	0.0	0.0	0.0	0.0	0.0	0
8.14	162	P	46.3	32.0	20.8	0.3	0.8	0.0	0.0	0.0	0.0	0.0	0.0	0.0	0.0	0.0	0.0	0
8.15	138	Sk	59.0	31.6	9.4	0.0	0.0	0.0	0.0	0.0	0.0	0.0	0.0	0.0	0.0	0.0	0.0	0
8.16	90	P	63.8	28.5	6.9	0.3	0.3	0.3	0.0	0.0	0.0	0.0	0.0	0.0	0.0	0.0	0.0	0
8.17	120	Sk	61.8	32.0	6.3	0.0	0.0	0.0	0.0	0.0	0.0	0.0	0.0	0.0	0.0	0.0	0.0	0
8.18	88	Sk	71.4	19.0	9.3	0.0	0.3	0.0	0.0	0.0	0.0	0.0	0.0	0.0	0.0	0.0	0.0	0
8.19	150	Sm	62.5	30.2	6.4	0.6	0.3	0.0	0.0	0.0	0.0	0.0	0.0	0.0	0.0	0.0	0.0	0
8.20	110	Sm	62.6	30.9	5.8	0.0	0.0	0.0	0.0	0.6	0.0	0.0	0.0	0.0	0.0	0.0	0.0	0
8.21	150	P	64.7	31.3	3.4	0.0	0.0	0.0	0.0	0.6	0.0	0.0	0.0	0.0	0.0	0.0	0.0	0
8.22	275	Sm	70.4	5.7	21.5	0.5	0.7	0.0	0.0	0.0	0.0	0.0	0.0	0.0	0.0	0.0	0.0	0
8.23	250	P	62.8	33.0	4.0	0.3	0.7	0.2	0.0	1.3	0.0	0.0	0.0	0.0	0.0	0.0	0.0	0
8.24	163	Sk	34.3	42.7	20.4	0.0	0.2	0.0	0.0	0.0	0.0	0.0	0.0	0.0	0.0	0.0	0.0	0
8.25	157	Sm	53.3	34.5	10.0	0.0	0.0	0.0	0.0	0.0	2.6	0.0	0.0	0.0	0.0	0.0	0.0	0
8.26	95	Sm	48.6	9.3	42.1	0.5	0.4	0.3	0.0	1.0	0.0	0.0	0.0	0.0	0.0	0.0	0.0	0
8.27	90	Sm	65.1	29.6	4.3	0.0	0.0	0.3	0.0	0.7	0.0	0.0	0.0	0.0	0.0	0.0	0.0	0
8.28	85	Cr	61.5	28.5	6.0	0.7	0.8	0.4	1.1	0.0	0.5	0.0	0.0	0.0	0.0	0.6	0.0	0
8.29	150	P	70.9	15.8	9.1	1.3	1.4	0.5	0.0	1.0	0.0	0.0	0.0	0.0	0.0	0.0	0.0	0
8.30	167	Sm	60.7	33.3	4.7	0.0	0.6	0.0	0.0	0.0	0.0	0.0	0.7	0.0	0.0	0.0	0.0	0
8.31	300	P	70.0	27.8	2.0	0.0	0.3	0.0	0.0	0.0	0.0	0.0	0.0	0.0	0.0	0.0	0.0	0
8.32	130	Sm	61.8	34.7	3.5	0.0	0.0	0.0	0.0	0.0	0.0	0.0	0.0	0.0	0.0	0.0	0.0	0
8.33	167	P	65.4	32.4	2.3	0.0	0.0	0.0	0.0	0.0	0.0	0.0	0.0	0.0	0.0	0.0	0.0	0
8.34	140	P	60.4	33.8	3.2	1.0	1.1	0.4	0.0	0.0	0.0	0.0	0.0	0.0	0.0	0.0	0.0	0
8.35	210	P	56.5	36.6	5.5	0.5	0.5	0.3	0.0	0.0	0.0	0.0	0.0	0.0	0.0	0.0	0.0	0
8.36	110	P	58.2	33.4	3.7	1.4	1.1	1.1	0.0	1.2	0.0	0.0	0.0	0.0	0.0	0.0	0.0	0
8.37	84	B	54.7	37.1	3.2	1.7	1.3	0.9	0.0	1.1	0.0	0.0	0.0	0.0	0.0	0.0	0.0	0
8.38	125	Sm	41.0	36.9	7.2	4.7	0.0	2.8	0.0	0.9	0.0	0.0	0.0	0.0	0.0	1.3	4.9	0.3
8.39	65	P	53.8	31.9	6.3	0.0	0.2	0.3	2.9	0.7	1.1	2.6	0.0	0.2	0.0	0.0	0.0	0
8.40	75	Sm	57.3	31.7	4.8	0.0	0.0	0.4	0.6	0.7	0.3	4.3	0.0	0.0	0.0	0.0	0.0	0
8.41	82	Fs	59.0	27.7	5.2	0.3	0.4	0.0	2.5	0.8	1.1	2.8	0.0	0.0	0.3	0.0	0.0	0
8.42	100	Fs	59.5	34.3	4.2	0.4	0.4	0.4	0.0	0.8	0.0	0.0	0.0	0.0	0.0	0.0	0.0	0
8.43	85	P	49.5	36.1	9.4	0.3	0.7	0.3	2.1	0.9	0.9	0.0	0.0	0.0	0.0	0.0	0.0	0
8.44	127	Sm	59.9	34.0	4.6	0.0	0.4	0.0	0.9	0.0	0.2	0.0	0.0	0.0	0.0	0.0	0.0	0
8.45	180	P	61.1	34.6	4.4	0.0	0.0	0.0	0.0	0.0	0.0	0.0	0.0	0.0	0.0	0.0	0.0	0
8.46	130	Mx	59.1	30.1	9.6	0.3	0.3	0.0	0.0	0.7	0.0	0.0	0.0	0.0	0.0	0.0	0.0	0
8.47	171	P	67.7	28.8	3.4	0.5	0.3	0.3	0.0	0.0	0.0	0.0	0.0	0.0	0.0	0.0	0.0	0
8.48	127	P	61.6	33.2	4.1	0.0	0.0	0.4	0.0	0.7	0.0	0.0	0.0	0.0	0.0	0.0	0.0	0
8.49	147	P	53.7	29.3	14.7	0.4	0.5	1.6	0.0	0.0	0.0	0.0	0.0	0.0	0.0	0.0	0.0	0
8.50	137	Sk	66.5	27.0	6.5	0.0	0.0	0.0	0.0	0.0	0.0	0.0	0.0	0.0	0.0	0.0	0.0	0
8.51	185	Sm	59.9	26.0	8.7	0.8	2.7	0.3	0.0	0.7	0.0	0.0	0.0	0.0	0.0	1.0	0.0	0
8.52	187	Sm	60.3	26.2	9.5	1.0	2.0	0.0	0.0	0.0	0.0	0.0	0.0	0.0	0.0	1.0	0.0	0
8.53	197	P	63.4	32.5	4.1	0.0	0.0	0.0	0.0	0.0	0.0	0.0	0.0	0.0	0.0	0.0	0.0	0
8.54	111	P	66.4	30.1	3.5	0.0	0.0	0.0	0.0	0.0	0.0	0.0	0.0	0.0	0.0	0.0	0.0	0
8.55	95	Sm	57.6	29.5	10.0	1.4	0.5	0.3	0.0	0.7	0.0	0.0	0.0	0.0	0.0	0.0	0.0	0
8.56	75	P	62.7	27.0	8.6	0.4	0.4	0.0	0.0	0.9	0.0	0.0	0.0	0.0	0.0	0.0	0.0	0
8.57	127	Sm	55.1	8.8	28.6	0.5	0.4	0.3	0.0	1.7	0.0	0.0	0.0	0.0	0.0	0.0	4.2	0.4
8.58	147	P	64.5	29.1	4.7	0.0	0.6	0.0	0.0	0.7	0.0	0.0	0.4	0.0	0.0	0.0	0.0	0
8.59	180	P	52.4	37.2	8.2	0.6	0.8	0.8	0.0	0.0	0.0	0.0	0.0	0.0	0.0	0.0	0.0	0
8.60	160	Sk	54.3	40.4	4.6	0.0	0.0	0.8	0.0	0.0	0.0	0.0	0.0	0.0	0.0	0.0	0.0	0
8.61	152	Sk	63.2	32.4	4.3	0.0	0.0	0.4	0.0	0.0	0.0	0.0	0.0	0.0	0.0	0.0	0.0	0
8.62	168	P	64.8	30.0	4.8	0.0	0.4	0.0	0.0	0.0	0.0	0.0	0.0	0.0	0.0	0.0	0.0	0
8.63	160	Sk	62.8	33.8	3.2	0.0	0.2	0.0	0.0	0.0	0.0	0.0	0.0	0.0	0.0	0.0	0.0	0
8.64	140	P	63.6	31.2	4.5	0.0	0.0	0.7	0.0	0.0	0.0	0.0	0.0	0.0	0.0	0.0	0.0	0
8.65	100	P	52.7	23.9	22.0	0.4	0.4	0.0	0.0	0.6	0.0	0.0	0.0	0.0	0.0	0.0	0.0	0

P = polygonal; Sk = skein; Sm = smooth; B = brain; Cr = crossed; Mx = mixed; Fs = fish scale.

Genge and Grady (1999) proposed the occurrence of four main processes during the entry stage due to heating of meteorites. The first chemical and mineralogical reaction of crust fusion involves the separation of Fe-rich liquids and subsequent reaction with atmospheric oxygen. Meteorite ablation spheres are melt droplets that separate from meteoroids by ablation during atmospheric entry. These spheres removed during the last few seconds of luminous flight must have been derived from the same melt that cooled to form the melted crust. Low-altitude meteoritic ablation microspherules could be locally abundant on the Earth's surface. It

Please cite this article in press as: Orgeira, M.J., et al., Extraterrestrial microspherules from Bajada del Diablo, Chubut, Argentina, Geoscience Frontiers (2016), http://dx.doi.org/10.1016/j.gsf.2016.01.004

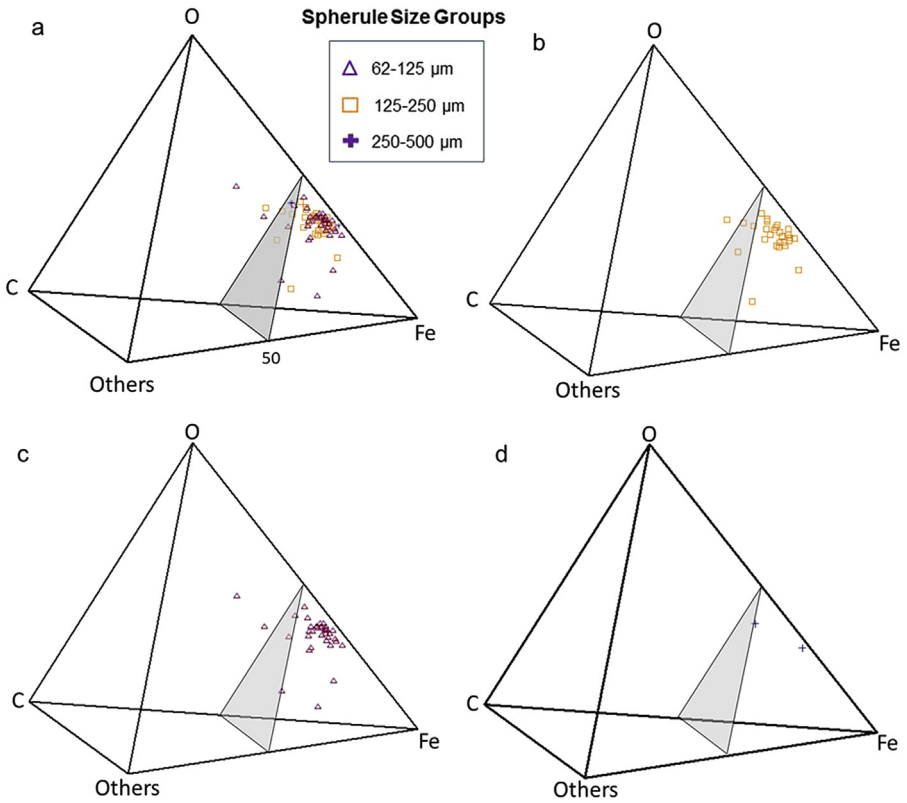

Figure 11. Chemical composition of the collected microspherules sorted by size. a: All size groups. b: 125–250 μm spherules. c: 62–125 μm spherules. d: 250–500 μm spherules. No significant variation in composition related to size has been detected.

is important to distinguish them from cosmic spherules, which form by the melting of extraterrestrial dust particles, because they could severely bias individual collections of micrometeorites. Meteorite ablation microspherules can be unequivocally identified based on their cosmogenic isotope determination because, as part of a larger meteoroid, they experience less exposure to radiation than cosmic spherules.

Marini et al. (2004) found microspherules similar to those described in the present contribution. The inner parts of some of them consist of large, interlocking grains of magnetite. Frequently, inner structures comprise a central hollow. The walls of the cavity exhibit extremely coarse, dendritic clusters of magnetite-wüstite. According to these authors, the microspherules might record growth from a vapor phase, during the earliest sequences of an impact scenario, from entry into upper atmosphere to mass vapor release, immediately after impact.

Guaita and Martegani (2008) compared the mechanisms involved in analogous synthetic material with those of well established cosmic origin. Following these results, the origin of microspherules can only be explained as ablation products by aerodynamic melting of meteoroids where they enter into the atmosphere. Typical ablation spheres are produced by melting of

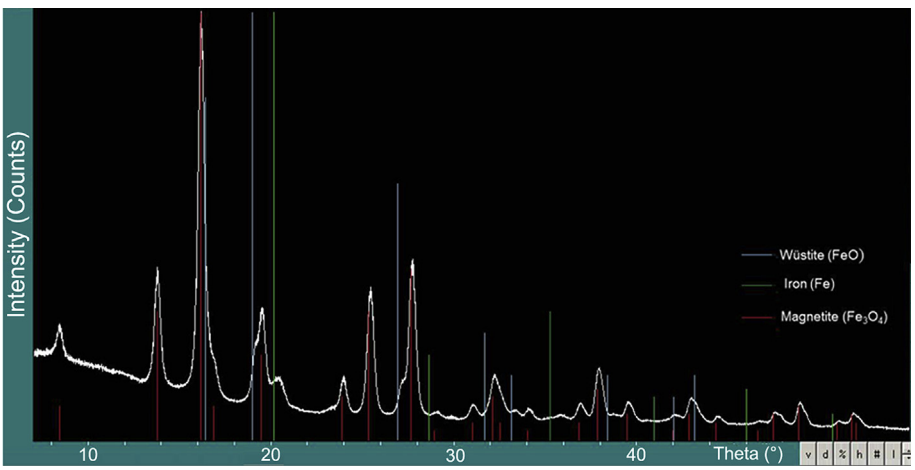

Figure 12. XRD data from microspherule 8.23. Main peaks obtained of the powder diagrams correspond to a major spinel phase (magnetite, PDF 19/0629). Additional signals at 19.18, 27.20, 33.29 and 42.22° could be assigned to wüstite (PDF 46-1312). Weak peak at 20.41° could indicate the presence of Fe° (PDF 87-0721).

Please cite this article in press as: Orgeira, M.J., et al., Extraterrestrial microspherules from Bajada del Diablo, Chubut, Argentina, Geoscience Frontiers (2016), http://dx.doi.org/10.1016/j.gsf.2016.01.004

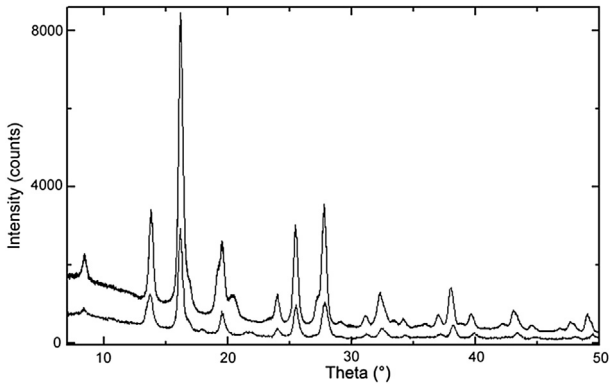

Figure 13. X-ray data from microsphere 8.23 and 8.24. Main peaks in both samples correspond to a major spinel phase (magnetite, PDF 19/0629). Sample 8.24 displayed weak and wide signals at 17.82 and 21.76° that were not present in sample 8.23; they were unable to be assigned.

cosmic dust and comets fragments which enter the atmosphere at high velocities. Therefore, approximately at 80 km altitude a deceleration, intense frictional heating, melting, partial vaporization and solidification take place.

Johnson and Melosh (2012) proposed a numerical model of spherule formation in an impact produced vapor plume. Their model shows that smaller spherules can be formed in the outer, faster moving, portions of the vapor plume at earlier times. Glass and Simonson (2012) also proposed that during large impacts, layers of melted and crushed rock are spread over large areas. At distances greater than ~10 crater *radii*, the distal ejecta primarily consist of impact microspherules formed from melt and vapor-condensate droplets. Johnson and Melosh (2014) developed a refined numerical model of microspherules formation. Their analysis makes predictions about the size of the ejecta products and their relationship to impactor size, impact velocity and ejection velocity. Larger impactor sizes resulted in larger ejecta products and higher ejection velocities resulted in smaller ejecta ones.

Ni-rich iron metal nuggets can occur within microspherules. I-type microspherules often contain a single large spherical void that may form by the loss of molten metal beads from the particle (Genge et al., 2008). They can also exhibit a central irregular void space, probably due to a rapid cooling of the melt inwards the surface.

Furthermore, Bi et al. (1993) suggested that Ni-Fe alloy microspherules represent the ejected cores of cosmic spherules. They described qualitatively the complete process as the result of which a FeO crust spherule without core is formed. Yada et al. (1996) found two types of internal composition in I-type magnetic microspherules collected from deep sea sediments. One of these with a Ni-free Fe-oxide crust accompanied with a Fe-Ni off-centered core and the other without a core surrounded by a Fe oxide crust. Based on numerical simulations, they proposed that this differentiation took place during the entrance of particles in the atmosphere with link to an ablation process where oxidation has a primary role, similar to those described by Bi et al. (1993).

Considering the different hypotheses proposed above, we infer that the *Crater 8* microspherules might have been generated by the ablation of an extraterrestrial body during its entry into the atmosphere (Blanchard et al., 1978, among others), or by a plume linked with the high speed impact of a discrete body taking into consideration individual spherule sizes (Johnson and Melosh, 2014). Currently, no isotopic data is available in order to reinforce the meteoric origin of the studied material.

The chemical composition and hollow structure displayed by several *Crater 8* microspherules (Tables 1–3, and Fig. 7) could be attributed to a loss of a Ni-Fe core, like the one underwent by the microspherules described by Bi et al. (1993).

The presence of peduncles whose composition differs from the associated microspherules (Table 1 and Fig. 6) could be explained through a differentiation process during crystallization. The original fluid would have segregated in a first stage mainly forming Fe-O microspherules and then a residual higher silica fluid crystallized as a peduncle.

Considering *Crater 8* dimensions and the associated crater strewn field dispersion, we can draw the following inferences. The apparent depth/diameter ratios of individual structures in Bajada del Diablo is not consistent with the relationship proposed by Pike (1980) and Grieve and Pilkington (1996) or the geometry of undisturbed simple craters like Kamil Crater described by Folco et al. (2011). Furthermore, the crater strewn field of Bajada del Diablo does not show the expected dispersion size according to Collins et al. (2005). Also, there is a significant variability among the morphometric parameters of currently known strewn fields. However, given the fact that the accepted strewn fields are relatively few, and the majority of them were modified by exogenous processes, the preservation of only a partial signature of the original geometry ratios seems to be frequent.

The criteria established by French and Koeberl (2010) for description and recognition of terrestrial impact structures have not been satisfied yet for Bajada del Diablo features. Nevertheless, these circular structures have three significant aspects: remarkably higher concentrations of microspherules than the average cosmic influx in the center of *Crater 8*; geophysical signatures compatible with the ones expected for an impact structures indicated by Prezzi et al. (2012, 2013, 2016), and geomorphological characteristics described by Acevedo et al. (2009, 2012). These lines of evidence merit further investigation as a potential candidate for impact structure research.

Table 2
EDS analysis of two broken microspherules taking into account different sample size areas for each specimen (Samples 8.36 and 8.66).

Sample	Area (μm^2)	Fe	O	C	Si	Ca	Al	Texture	Comments
8.66 (Inner)	10	71.9	14.2	12.7	0.3	0.3	0.2	Dendritic intergrowths	NE quadrant
8.66 (Inner)	10	69	25.1	3.4	0.9	0.6	0.8	Dendritic intergrowths	SW quadrant
8.36 (Inner)	0.16	73.1	9.4	17.3	0	0	0	Dendritic intergrowths	Center quadrant
8.36 (Inner)	5	68.4	20.9	10.5	0	0	0	Dendritic intergrowths	E quadrant
8.36 (Inner)	6.25	67.1	29.4	3.4	0	0	0	Dendritic intergrowths	SW quadrant

Weigh%.

5. Conclusions

Our study leads to the following major conclusions.

The microspherules seem to be generated as a byproduct of an asteroid entry into the atmosphere.

According to the chemical composition dominated by FeO, the *Crater 8* microspherules were classified as I-type. XRD and EMPA analyses show magnetite-wüstite and possible metallic iron intergrowths.

Three lines of evidence suggest that at least a part of the Bajada del Diablo area could have undergone multiple impacts of extraterrestrial impactors as follows: (1) The existence of circular structures that are not related to exogenous or volcanic processes;

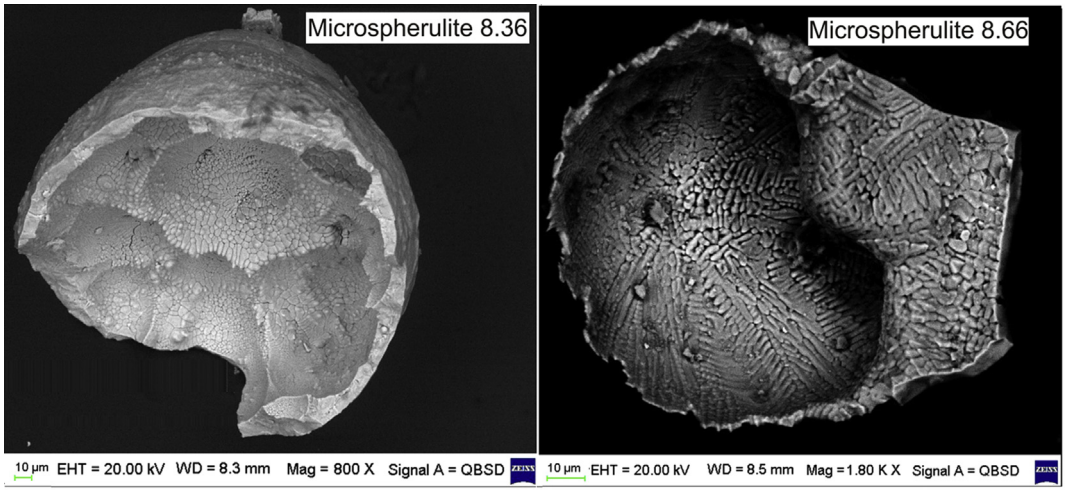

Figure 14. Internal structure observed with backscattered diffraction exhibit a polygonal patterned surface that is compatible with a dendritic crystal intergrowth.

Table 3
EMPA determinations from two spherules (five measurements in total, two from one and three from the other one).

	Msph 1-1		Msph 1-2		Microsph 2-1		Msph 2-2		Msph 2-3	
	wt.%	σ	wt.%	σ	wt.%	σ	wt.%	σ	wt.%	σ
Al	0.036	0.02	0.016	0.02	0.103	0.01	0.046	0.02	0.072	0.01
Si	0.045	0.02	0.027	0.02	0.052	0.01	0.033	0.02	0.026	0.02
Mg	bdl		0.007	0.02	0.026	0.01	0.001	0.01	0.007	0.01
Co	bdl		bdl		bdl		bdl		bdl	
Ca	bdl		bdl		bdl		bdl		bdl	
Ti	bdl		bdl		0.082	0.06	0.09	0.10	0.09	0.10
Pt	bdl		bdl		0.178	0.08	0.032	0.11	bdl	
Ir	bdl		bdl		0.05	0.07	0.066	0.12	0.008	0.10
Os	bdl		0.145	0.12	bdl		bdl		0.036	0.13
Ni	bdl		0.045	0.06	bdl		bdl		bdl	
Fe	100.692	0.05	101.897	0.08	100.144	0.04	101.233	0.05	100.497	0.05
Cr	0.042	0.04	0.019	0.04	0.037	0.03	0.003	0.04	0.012	0.04
Ru	0.055	0.04	bdl		bdl		0.046	0.04	bdl	
Rh	bdl		bdl		bdl		bdl		bdl	
Pd	bdl		bdl		bdl		bdl		bdl	
Total	100.87		102.15		100.67		101.55		100.74	

bdl = below detection limit; σ = standard deviation; Msph = microspherule

(2) magnetic, gravimetric and electrical resistivity anomalies compatible with the ones expected for impact; (3) the presence of meteoritic microspherules in anomalously high concentration.

Acknowledgments

We extend our most sincere thanks for the relevant suggestions and corrections to Dr. Luigi Folco and an anonymous reviewer. We also thank Mr. Eduardo Llambias for his invaluable assistance during the preparation of microspherules sections.

We also thank the University of Buenos Aires and Consejo Nacional de Investigaciones Científicas y Técnicas, Argentina. This work was carried out under Project UBACyT 20020130100146/14X236, PIP 00416/11 and PICT 2013-1950.

Appendix 1. Supplementary data

Supplementary data related to this article can be found online at http://dx.doi.org/10.1016/j.gsf.2015.10.004.

References

Acevedo, R.D., Ponce, J.F., Rocca, M., Rabassa, J., Corbella, H., 2009. Bajada del Diablo impact crater-strewn field: the largest crater field in the Southern Hemisphere. Geomorphology 110 (3–4), 58–67.

Acevedo, R.D., Rabassa, J., Ponce, J.F., Martínez, O., Orgeira, M.J., Prezzi, C., Corbella, H., González-Guillot, M., Rocca, M., Subías, I., Vásquez, C., 2012. The Bajada del Diablo astrobleme-strewn field, central Patagonia Argentina: extending the exploration to surrounding areas. Geomorphology 169, 151–164.

Alonso-Zarza, A.M., Wright, V.P., 2010. Calcretes. In: Alonzo-Zarza, A.M., Tanner, L.H. (Eds.), Carbonates in Continental Settings: Facies, Environments, and Processes. Developments in Sedimentology, vol. 61, pp. 225–268.

Ardolino, A.A., 1981. El vulcanismo cenozoico del borde suroccidental de la meseta de Somún Curá, provincia del Chubut. In: Proc. 7 Congreso Geológico Argentino, vol. 3, pp. 7–23. Buenos Aires. (in Spanish).

Ardolino, A.A., 1987. Descripción Geológica de la Hoja 42f. Sierra de Apas, Provincia de Chubut. Servicio Geológico Nacional. Dirección Nacional de Minería y Geología, Buenos Aires, 91 pp (in Spanish).

Ardolino, A.A., Franchi, M., 1996. Hoja Geológica 4366–1. Telsen. Dirección Nacional del Servicio Geológico, Subsecretaría de Minería de la Nación, Buenos Aires. Boletín 215. 110 pp (in Spanish).

Bi, D., Morton, R.D., Wang, K., 1993. Cosmic nickel-iron alloy spherules from Pleistocene sediments, Alberta, Canada. Geochimica et Cosmochimica Acta 5716, 4129–4136 (in Spanish).

Blanchard, M.B., Brownlee, D.E., Bunch, T.E., Hodge, P.W., Kyte, F.T., 1978. Meteor ablation spheres from deep-sea sediments. NASA Technical Memorandum 78510, 41 pp.

Bouza, P.J., 2012. Génesis de las acumulaciones de carbonatos en Aridisoles nordpatagónicos: su significado paleopedológico. Revista de la Asociación Geológica Argentina 69 (2), 300–315.

Carracedo Sánchez, M., Sarrionandia, F., Arostegui, J., Gil Ibarguchi, J.I., 2015. Silicate glass micro and nanospherules generated in explosive eruptions of ultrabasic magmas: implications for the origin of pelletal lapilli. Journal of Volcanology and Geothermal Research 293, 13–24.

Collins, G.S., Melosh, H.J., Marcus, R.A., 2005. Earth impact effects program: a web-based computer program for calculating the regional environmental

consequences of a meteoroid impact on Earth. Meteoritics & Planetary Science 406, 817–840.
Dunlop, D.J., Özdemir, O., 1997. Rock Magnetism: Fundamentals and Frontiers. Cambridge University Press, Cambridge, U.K., 565 pp.
Evans, M., Heller, F., 2003. Environmental Magnetism: Principles and Applications of Environmagnetics. Academic Press. Chapter 10(86), 299 pp.
Folco, L., D'Orazio, M., Fazio, A., Cordier, C., Zeoli, A., Ginneken, M., El-Barkooky, A., 2015. Microscopic impactor debris in the soil around Kamil crater (Egypt): inventory, distribution, total mass, and implications for the impact scenario. Meteoritics & Planetary Science 50 (3), 382–400.
Folco, L., Di Martino, M., El Barkooky, A., D'Orazio, M., Lethy, A., Urbini, S., Nicolosi, I., Hafez, M., Cordier, C., van Ginneken, M., Zeoli, A., Radwan, A.M., El Khrepy, S., El Gabry, M., Gomaa, M., Barakat, A.A., Serra, R., El Sharkawi, M., 2011. Kamil crater Egypt: ground truth for small-scale meteorite impacts on Earth. Geology 392, 179–182.
French, B.M., 1998. Traces of Catastrophe: a Handbook of Shock-metamorphic Effects in Terrestrial Meteorite Impact Structures. LPI Contribution No. 954. Lunar and Planetary Institute, Houston, 120 pp.
French, B.M., Koeberl, C., 2010. The convincing identification of terrestrial meteorite impact structures: what works, what doesn't, and why. Earth-Science Reviews 981, 123–170.
Genge, M.J., Grady, M.M., 1999. The fusion crusts of stony meteorites: implications for the atmospheric reprocessing of extraterrestrial materials. Meteoritics & Planetary Science 343, 341–356.
Genge, M.J., Engrand, C., Gounelle, M., Taylor, S., 2008. The classification of micrometeorites. Meteoritics & Planetary Science 433, 497–515.
Glass, B.P., Simonson, B.M., 2012. Distal impact ejecta layers: spherules and more. Elements 81, 43–48.
González Díaz, E., Malagnino, E.C., 1984. Geomorfología. In: Relatorio IX Congreso Geológico Argentino. Buenos Aires, pp. 347–364 (in Spanish).
Grieve, R.A.F., Pilkington, M., 1996. The signature of terrestrial impacts. AGSO Journal of Australian Geology and Geophysics 164, 399–420.
Guaita, C., Martegani, F., 2008. Cosmic microsphere: a SEM study. Memorie della Societa Astronomica Italiana Supplementi 12, 110.
Gurov, E.P., Gurova, E.P., 1998. The group of Macha craters in western Yakutia. Planetary and Space Science 462, 323–328.
Hay, R.L., Wiggins, B., 1980. Pellets, ooids, sepiolite and silica in three calcretes of de southwestern United States. Sedimentology 27, 559–576.
Johnson, B.C., Melosh, H.J., 2012. Formation of spherules in impact produced vapor plumes. Icarus 2171, 416–430.
Johnson, B.C., Melosh, H.J., 2014. Formation of melt droplets, melt fragments, and accretionary impact lapilli during a hypervelocity impact. Icarus 228, 347–363.
Maher, B.A., Thompson, R., Hounlow, M.W., 1999. In: Maher, B.A., Thompson, R. (Eds.), Quaternary Climates, Environments and Magnetism, (Chapter 1). Cambridge University Press, 390 pp.
Marini, F., Raukas, A., Tiirmaa, R., 2004. Magnetic fines from the Kaali impact-site (Holocene, Estonia): Preliminary SEM investigation. Geochemical Journal 38 (2), 107–120.
Narayan, D., Tandon, S., 1981. Calcrete conglomerate, case - hardened conglomérate and cornstone, Siwalik Group, Punjab, India. Sedimentology 28, 353–367.
Pike, R.J., 1980. Control of crater morphology by gravity and target type-Mars, Earth, Moon. In: Proc. Lunar and Planetary Science Conference, vol. 11, pp. 2159–2189.
Prezzi, C., Orgeira, M.J., Acevedo, R.D., Ponce, J.F., Martínez, O., Rabassa, J., Corbella, H., Vásquez, C., González, M., Subías, I., 2012. Geophysical characterization of two circular structures at Bajada del Diablo Patagonia, Argentina: indication of impact origin. Physics of the Earth and Planetary Interiors 192–193, 21–34.
Prezzi, C., Orgeira, M.J., Acevedo, R., Ponce, F., Martínez, O., Sarnataro, A., Rabassa, J., 2013. Bajada del Diablo Circular Structures Chubut, Argentina: Ground Gravity, Magnetic and Electromagnetic Surveys. Latinmag 3 Reunión Bienal de la Asociación Latinoamericana de Paleomagnetismo y Geomagnetismo, Montevideo, Uruguay. Latinmag Letters, 3: 3 2013, OA7, 1-6.
Prezzi, C., Orgeira, M.J., Martinez, O., Acevedo, R.D., Ponce, F., Goldmann, G., Magneres, I., Rabassa, J., 02/2016. Circular structures of Bajada del Diablo Argentina: geophysical signature compatible with an impact origin. Geophysical Journal International. http://dx.doi.org/10.1093/gji/ggw053 (accepted).
Raukas, A., 2004. Distribution and composition of impact and extraterrestrial spherules in the Kaali area Island of Saaremaa, Estonia. Geochemical Journal 382, 101–106.
Rochette, P., Folco, L., Suavet, C., Van Ginneken, M., Gattacceca, J., Perchiazzi, N., Braucher, R., Harvey, R.P., 2008. Micrometeorites from the transantarctic mountains. Proceedings of the National Academy of Sciences of the United States of America 10547, 18206–18211.
Stankowski, W.T.J., Katrusiak, A., Budzianowski, A., 2006. Crystallographic variety of magnetic spherules from Pleistocene and Holocene sediments in the Northern foreland of Morasko-Meteorite Reserve. Planetary and Space Science 541, 60–70.
Taylor, S., Lever, J.H., Harvey, R.P., 2000. Numbers, types, and compositions of an unbiased collection of cosmic spherules. Meteoritics & Planetary Science 55, 651–666.
Valencio, D.A., Orgeira, M.J., Bobbio, M.L., 1987. Magnetoestratigraphy and magnetic susceptibility data of the late Cenozoic Ensenadense and Bonaerense of the cities of Buenos Aires and La Plata, central-eastern Argentina. Quaternary of South America and Antartic Peninsula 5, 5–32.
Voldman, G.G., Genge, M.J., Albanesi, G.L., Barnes, C.R., Ortega, G., 2013. Cosmic spherules from the Ordovician of Argentina. Geological Journal 482 (3), 222–235.
Wright, V., 1983. A rendzina from de Lower Carboniferous of South Wales. Sedimentology 30, 159–179.
Yada, T., Nakamura, T., Sekiya, M., Takaoka, N., 1996. Formation processes of magnetic spherules collected from deep-sea sediments-observations and numerical simulations of the orbital evolution. Antarctic Meteorite Research 9, 218.

Please cite this article in press as: Orgeira, M.J., et al., Extraterrestrial microspherules from Bajada del Diablo, Chubut, Argentina, Geoscience Frontiers (2016), http://dx.doi.org/10.1016/j.gsf.2016.01.004